

Supplement of Biogeosciences Discuss., 11, 16527–16572, 2014
<http://www.biogeosciences-discuss.net/11/16527/2014/>
doi:10.5194/bgd-11-16527-2014-supplement
© Author(s) 2014. CC Attribution 3.0 License.



Supplement of

Predicting the denitrification capacity of sandy aquifers from in situ measurements using push-pull ^{15}N tracer tests

W. Eschenbach et al.

Correspondence to: W. Eschenbach (wolfram.eschenbach@ti.bund.de)

S1 In situ isotope analysis using MIMS

55 At two multilevel wells in the Fuhrberger Feld aquifer (FFA) (multilevel well B1 and B2) the concentration of ^{15}N labelled denitrification products in the sampled tracer solution was measured during the conducted push-pull tests directly in the field, using a membrane inlet mass spectrometer (MIMS) as described in Eschenbach and Well (2011). These measurements were done to compare online field MIMS measurements with the offline
60 laboratory analysis by isotope ratio mass spectrometry (IRMS) as described in section 2.5.1. The instrumental set up was similar to the laboratory setup described in Eschenbach and Well (2011) and installed inside a van. Briefly, it consisted of the quadrupole mass spectrometer a cryotrap, a membrane inlet, a cryostatic water bath, 2 peristaltic pumps, a reduction furnace and a T-connection.

65 After injection of tracer solution into the respective depths of the monitoring wells, samples of the tracer solution were extracted using a peristaltic pump (masterflex COLE-Parmer, Vernon Hills, USA) (see section 2.2). A subsample of the sampled tracer solution was then pumped through a T-connection using a second peristaltic pump (ISMATEC, BVP-Standard, Wertheim-Mondfeld, Germany). The T-connection was directly connected via stainless steel
70 tubing with the membrane inlet of the mass spectrometer (described in detail in Eschenbach and Well (2011)). The dissolved gasses in the sampled tracer solution diffused in the membrane inlet through the gas permeable membrane into the high vacuum of the mass spectrometer. A copper reduction furnace and a cryotrap were placed in the vacuum line between membrane inlet and the ion source of the mass spectrometer. N_2O was reduced to N_2
75 within the reduction furnace. Therefore ^{15}N labelled denitrification derived N_2 and N_2O was analyzed as $(\text{N}_2+\text{N}_2\text{O})$ on the molecular ion masses 28, 29 and 30 as $^{28}\text{N}_2$, $^{29}\text{N}_2$ and $^{30}\text{N}_2$. The cryotrap was filled with liquid N_2 in order to remove water vapour and CO_2 (see also Fig. 1 Analyser side, in Eschenbach and Well (2011)). The membrane inlet and a flask containing air-equilibrated standard water were placed within a cryostatic water bath (Thermo Haake,
80 HAAKE AG, Karlsruhe, Germany) to ensure constant membrane inlet, sample and air-equilibrated standard water temperatures. The air-equilibrated standard water was manufactured as described in Kana et al. (1994) and used to calibrate the MIMS.

5 push-pull tests (at multilevel well B1 and at B2, respectively) with parallel online MIMS measurements were conducted, in the depths of 7, 8 (B1) and 8, 9 and 10 m (B2) below soil
85 surface (Table 1). Overall, there were 58 pairs of IRMS and MIMS measurements. Both online field MIMS and offline laboratory IRMS measurement were in close agreement

(Fig. S1). The averaged concentrations of the sum of ^{15}N labelled denitrification derived N_2 and N_2O ($(\text{N}_2+\text{N}_2\text{O})_{\text{den}}$) measured with both methods ranged from 0.9 to 99 and 0.3 to $16 \mu\text{g N l}^{-1}$, in samples from B1 and B2 respectively. Maximal differences between MIMS and IRMS measurements of $(\text{N}_2+\text{N}_2\text{O})_{\text{den}}$ were 6.6 and $2.5 \mu\text{g N l}^{-1}$ for samples from B1 and B2 respectively (Fig. S2).

The Bland-Altman-method for method comparison was used to evaluate the agreement of both methods (Bland and Altman, 1986) because correlation and regression analysis can result in the context of method comparison to significant misinterpretations (Altman and Bland, 1983; Bland and Altman, 2003, 1995, 1986). Denoting the results of the IRMS and MIMS measurement of $(\text{N}_2+\text{N}_2\text{O})_{\text{den}}$, as $(\text{N}_2+\text{N}_2\text{O})_{\text{IRMS}}$ and $(\text{N}_2+\text{N}_2\text{O})_{\text{MIMS}}$, respectively. The differences between measurements of individual samples with both methods [$(\text{N}_2+\text{N}_2\text{O})_{\text{IRMS}} - (\text{N}_2+\text{N}_2\text{O})_{\text{MIMS}}$] were plotted against the average of both measurements [$(\text{N}_2+\text{N}_2\text{O})_{\text{IRMS}} + (\text{N}_2+\text{N}_2\text{O})_{\text{MIMS}}/2$] (Fig. S2). Furthermore the average of differences (\bar{d}), the 95 %-limits of method agreement and 95 %-confidence intervals were calculated as described in Bland and Altman (1986).

The distribution of the magnitude of differences in Figure S2 suggests that there is no substantial increase in variance between both methods with increasing magnitude of measurement, which is a prerequisite for the calculation of method bias and 95 %-limits of method agreement without the need of transforming the data. The average of differences (\bar{d}) of all parallel measurements (= estimated method bias) was rather small ($\bar{d}= 0.6 \mu\text{g N l}^{-1}$; Fig. S2). The 95 %-limits of method agreement calculated as described in Bland and Altman (1986) were $\bar{d}\pm 4 \mu\text{g N l}^{-1}$. This means that 95 % of observed differences are expected to fall within these limits. The confidence bands for (\bar{d}) and the 95 %-limits of method agreement are narrow (Fig. S2) with values of $\bar{d}\pm 0.46$ and 95 %-limits $\pm 0.8 \mu\text{g N l}^{-1}$, respectively, showing that sample size was sufficient for the calculation of relative precise values for the estimated method bias and estimated limits of method agreement.

The comparison of online field measurements using MIMS with laboratory offline measurements (IRMS) thus showed a good agreement between both methods (Figs. S1 and S2) with only minor bias under the experimental conditions such as those encountered during this study, i.e. were $(\text{N}_2+\text{N}_2\text{O})_{\text{den}}$ was in the range of 0.9 to $99 \mu\text{g N l}^{-1}$ and ^{15}N abundances of denitrified NO_3^- were between 45 and 60 atom % ^{15}N . This close agreement is in line with our previous study where offline IRMS and online MIMS measurement were compared under laboratory conditions (Eschenbach and Well, 2011). This shows that in situ application does not alter the precision of the MIMS system.

In summary, the MIMS system was suitable for isotope analysis precise enough for the full range of measured concentrations, showing that this analytical system is suitable for in situ analysis during ^{15}N push pull tests. The main advantages with respect to the conventional IRMS approach is that results can be obtained in the course of experiments directly in the field. Sampling intervals can thus be adapted to get more precise rates. Moreover, the length of the pull phase can be limited to the duration of clearly increasing $(\text{N}_2+\text{N}_2\text{O})_{\text{den}}$ concentrations to save working time. Finally, the relatively low cost and simple handling of the MIMS system are favourable to enable extensive application of the ^{15}N push-pull approach to explore denitrification capacities of aquifers.

130

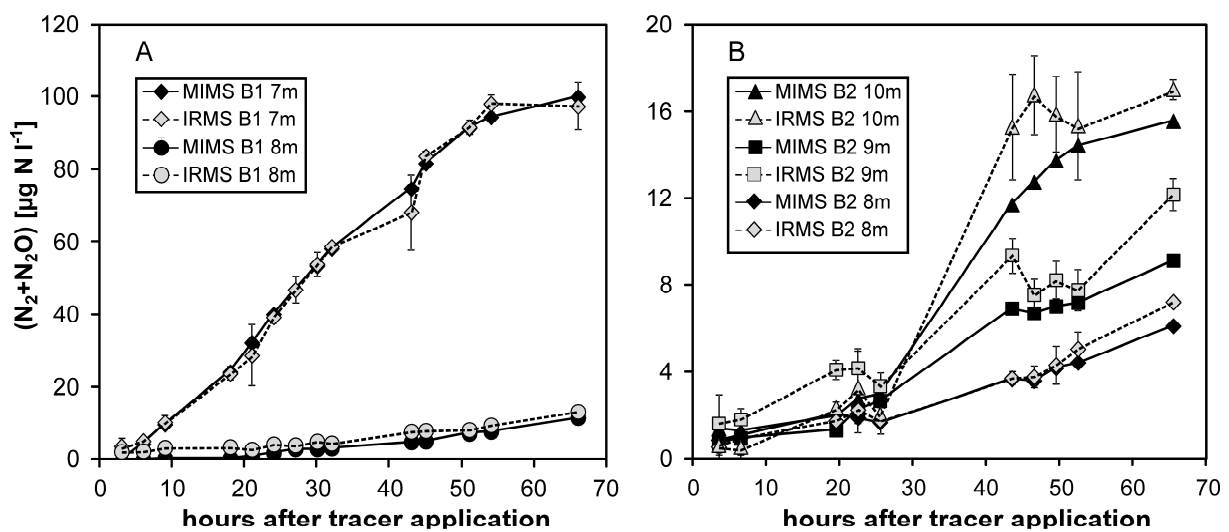


Fig. S1. Comparison of online field measurements of $(\text{N}_2+\text{N}_2\text{O})_{\text{den}}$ from aqueous samples, using a membrane inlet mass spectrometer (MIMS) with standard offline laboratory measurements by means of isotope ratio mass spectrometry (IRMS) at the multilevel wells B1 (A) and B2 (B) for 5 ^{15}N push-pull tracer tests in the Fuhrberger Feld Aquifer.

140

145

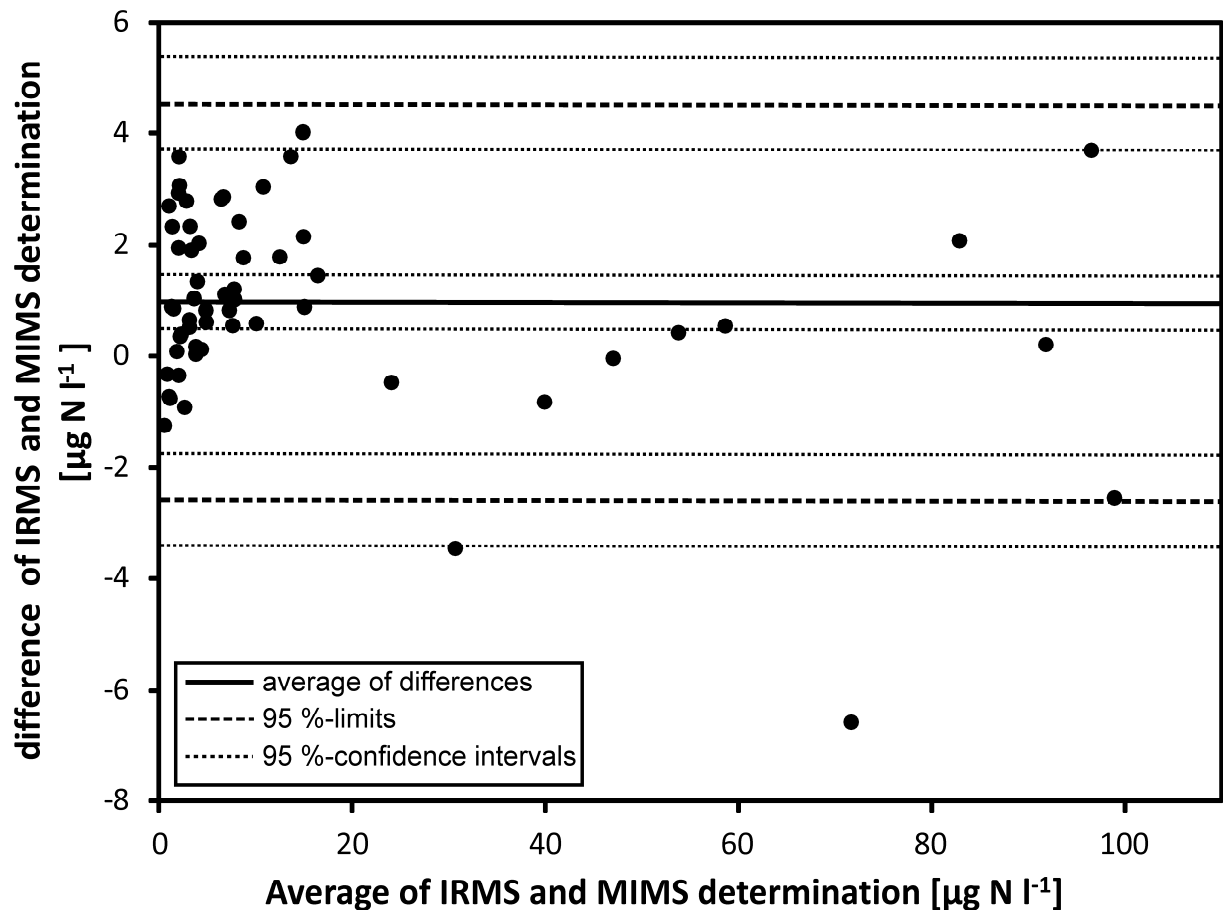


Fig. S2. Bland-Altman-Plot of the differences between online field MIMS analysis and offline laboratory IRMS measurement plotted against the average of both determinations.

150

S2 Possible confounding factors and uncertainties

Addy et al. (2002) discussed 3 potential confounding factors for the quantification of ^{15}N gas formation during push-pull tests: (i) dilution of denitrification derived gases, (ii) degassing of ^{15}N labelled denitrification derived gasses during the pull-phase of ^{15}N tracer tests (see therefore also discussion in Eschenbach and Well (2011)) and (iii) a lag phase between ^{15}N tracer injection and microbial response. In the following it is briefly referred to (iii).

Microbial adaptation processes after ^{15}N tracer injection might require time especially in the NO_3^- -free zone of aquifers (see Sect. 4.2), where aquifer material is brought into contact with NO_3^- for the first time. After pre-conditioning a clear lag phase was not observed during push-pull tests in the NO_3^- -free zone at multilevel well B4 in the FFA, therefore it is believed that this is attributed to the stimulation of denitrifiers due to the repeated injections of NO_3^- enriched groundwater at this multilevel well. Therefore, pre-conditioning might be a way to shorten or eliminate the observed lag phases between tracer injections and microbial response.

165

An additional uncertainty during push-pull tests (iv) is the effective porosity of investigated aquifer sediments. The effective porosity determines the volume of aquifer solids in reaction contact with 1 L test solution. Therefore, this value is needed to relate concentration data of evolved $(\text{N}_2+\text{N}_2\text{O})_{\text{den}}$ from $(\mu\text{g N L}^{-1})$ to $(\mu\text{g N kg}^{-1})$. This conversion strongly increases the coefficient of variation (CV) of concentration measurements of $(\text{N}_2+\text{N}_2\text{O})_{\text{den}}$ and thus increases the uncertainty of measured $D_r(\text{in situ})$ because of the uncertainty of the real effective porosity of the tested aquifer material (see Sect. 2.7). The effective porosity at the injection point can be measured with pumping tests prior or after the push-pull ^{15}N tracer test to reduce this source of uncertainty.

170

175

180

185

190

195

200

205

210

215

S 3. Additional detailed results from laboratory incubations and linear regression models

Table S1. Denitrification rates, cumulative denitrification, stock of reduced compounds, sulphate formation capacity and estimated minimal lifetime of denitrification of incubated samples from both aquifers (Eschenbach and Well, 2013) and corresponding in situ denitrification rates.

Sample location	Depth interval m	Aquifer zone ^a	$D_{cum}(365)^b$ mg N kg ⁻¹ yr ⁻¹	SRC ^c			SFC ^f mg S kg ⁻¹ yr ⁻¹	D_r (in situ) μg N kg ⁻¹ d ⁻¹
				SRC ^c	SRC _C ^d	SRC _S ^e		
FFA B1	6.0-7.0	transition zone	17.18	659.6	599.5	60.1	6.1	17.59
FFA B1	7.0-8.0	sulphidic	56.24	5974.2	5552.7	421.5	39.4	1.51
FFA B2	2.0-3.0	non-sulphidic	0.19	240.8	220.7	20.1	0.1	0.12
FFA B2	3.0-4.0	non-sulphidic	0.37	215.4	189.2	26.3	-0.1	0.12
FFA B2	4.0-5.0	non-sulphidic	4.34	540.2	508.0	32.2	1.0	0.07
FFA B2	8.0-9.0	transition zone	10.53	1638.2	1515.5	122.7	3.5	8.65
FFA B2	9.0-10.0	transition zone	12.68	610.7	502.0	108.7	2.2	8.65
FFA B4	7.0-8.0	sulphidic	20.16	603.6	450.2	153.4	9.6	2.76
FFA B4	8.0-9.0	sulphidic	34.09	1289.5	1038.9	250.7	22.0	2.28
FFA B6	2.0-3.0	non-sulphidic	2.64	687.0	648.9	39.1	0.3	0.06
FFA B6	3.0-4.0	non-sulphidic	1.46	1017.4	976.5	40.9	0.1	0.06
FFA N10	4.5-5.0	transition zone	8.69	1239.0	1204.1	34.8	1.5	12.89
FFA N10	5.0-5.5	transition zone	8.75	721.6	687.1	34.5	2.1	12.89
FFA N10	5.5-6.0	transition zone	7.82	674.6	640.3	34.3	5.2	12.89
FFA N10	7.7-8.3	transition zone	15.04	329.5	290.0	39.5	1.5	23.19
FFA N10	8.3-8.6	transition zone	15.17	331.5	298.7	32.9	6.9	23.19
FFA N10	10.0-10.4	sulphidic	17.45	320.6	289.3	31.3	5.4	-
FFA N10	10.4-10.7	sulphidic	50.07	5571.6	5247.7	323.9	9.4	-
FFA N10	12.0-13.0	sulphidic	52.84	2771.3	2381.7	389.6	37.9	-
FFA N10	13.0-14.0	sulphidic	38.04	2134.1	1723.3	410.8	18.2	-
FFA N10	16.0-17.0	sulphidic	46.65	2744.7	2431.5	313.2	23.6	-
FFA N10	17.0-18.0	sulphidic	46.55	2642.7	2335.0	307.8	36.8	-
GKA	8.0-9.0	non-sulphidic	0.63	132.6	95.0	37.6	0.9	0.00
GKA	9.0-10.0	non-sulphidic	0.34	97.1	70.7	26.4	0.4	0.00
GKA	22.0-23.0	non-sulphidic	1.57	193.3	164.2	29.1	0.2	0.00
GKA	23.0-24.0	non-sulphidic	2.83	204.5	179.2	25.3	-0.0	0.00
GKA	25.9-27.0	sulphidic	15.63	2857.4	2381.0	476.4	1.2	1.23
GKA	27.0-28.3	sulphidic	41.82	6634.0	5943.2	690.8	8.3	1.23
GKA	28.3-29.3	sulphidic	37.82	4495.6	3878.5	617.2	13.8	4.43
GKA	29.3-30.3	sulphidic	35.49	4766.8	4236.0	530.8	8.1	4.43
GKA	30.3-31.2	sulphidic	6.54	1086.9	731.4	355.4	3.8	0.50
GKA	31.3-32.0	sulphidic	4.09	1122.4	777.7	344.7	5.0	0.50
GKA	32.9-33.7	sulphidic	7.28	1206.0	765.6	440.4	10.2	0.50
GKA	33.7-34.7	sulphidic	12.25	1057.4	700.9	356.6	17.7	2.00
GKA	35.7-36.7	sulphidic	52.46	8861.3	8366.7	494.6	30.0	6.19
GKA	36.7-37.7	sulphidic	11.07	689.6	216.7	472.8	9.2	6.19
GKA	37.7-38.7	sulphidic	12.06	1347.7	1083.1	264.7	4.6	6.19
GKA	65.1-65.4	sulphidic	13.22	1441.2	941.3	499.9	1.3	2.27
GKA	67.1-67.5	non-sulphidic	8.18	471.0	333.8	137.2	1.3	2.27
GKA	67.5-68.0	non-sulphidic	8.11	487.1	351.5	135.6	0.7	2.27

FFA Fuhrberger Feld aquifer; GKA Großenkneten aquifer; ^a sediment characteristic; ^b cumulative denitrification after one year of incubation; ^c stock of reactive compounds (SRC); ^d fraction of organic carbon in the SRC; ^e fraction of total-S in the SRC; ^f sulphate formation capacity (SFC).

Table S2. Lambda values of the Box-Cox transformed $D_r(\text{in situ})$ and variables measured during anaerobic incubation.

Data set	Lamda values		
	$D_r(\text{in situ})$	$D_{\text{cum}}(365)$	SRC
Whole data set	0.216	0.303	-0.024
FFA	0.214	0.369	-0.185
GKA	0.257	0.236	0.039
non-sulphidic zone	0.041	0.122	1.493
Sulphidic zone	0.190	0.260	0.229
transition zone	-0.150	-0.029	-0.159
NO_3^- -bearing	0.099	0.337	0.797
NO_3^- -free	0.319	0.670	0.492

Table S3. Simple regressions between $D_r(\text{in situ})$ and individual sediment parameters from aquifer parallels. $f^{B-C}(X) = A + B \times f^{B-C}(D_r(\text{in situ}))$. For each sub data set the two sediment parameters with the best correlation coefficient with $D_r(\text{in situ})$ are listed.

Data set	X^a	N^b	A	B	R^c	R^2
Whole data set	SO_4^{2-}	29	3.697	-0.564	0.58	0.33
Whole data set	C_{org}	34	5.516	0.134	0.40	0.16
FFA	C_{hws}	14	19.74	1.754	0.75	0.56
FFA	SO_4^{2-}	11	3.263	-0.472	0.72	0.52
GKA	total-S	18	92.88	17.51	0.75	0.56
GKA	C_{org}	18	5.612	0.324	0.69	0.48
non-sulphidic	total-S	11	5.128	0.150	0.62	0.38
non-sulphidic	C_{org}	11	680.1	51.58	0.42	0.18
sulphidic	total-S	23	543.2	-109.7	0.69	0.48
sulphidic	SO_4^{2-}	18	3.540	-0.614	0.49	0.24
transition zone	total-S	8	0.608	-0.001	0.60	0.36
transition zone	C_{org}	8	5.341	-0.601	0.73	0.53
NO_3^- -bearing	C_{org}	17	151.0	12.75	0.55	0.30
NO_3^- -bearing	SO_4^{2-}	14	5.612	-0.501	0.53	0.28
NO_3^- -free	SO_4^{2-}	15	3.085	-0.844	0.51	0.26
NO_3^- -free	C_1	14	34.51	5.418	0.29	0.08

225 ^a Independent sediment parameter; ^b Sample number; ^c Correlation coefficient; SO_4^{2-} extractable sulphate-S; C_{hws} hot-water soluble organic carbon; C_1 KMnO_4 labile organic carbon; C_{org} total organic carbon; total-S total sulphur.

230

Table S4. Lambda values of the Box-Cox transformed sediment parameters.

Data set	Lamda values								
	$D_r(7)$	$D_{cum}(365)$	$D_r(\text{in situ})$	C_{org}	total-S	$SO_4^{2-}_{extr}$	DOC_{extr}	C_{hws}	C_l
Whole data set	0.487	0.303	0.216	-0.050	0.132	0.457	0.946	0.825	0.199
FFA	0.583	0.369	0.214	-0.191	-0.292	0.254	-	0.915	0.513
GKA	0.445	0.236	0.257	-0.052	0.685	0.628	-1.307	-0.203	0.291
non-sulphidic	-0.168	0.122	0.041	1.060	0.062	1.161	-	1.434	0.183
sulphidic	0.375	0.260	0.190	0.162	0.965	0.368	-1.931	1.314	-0.081
transition zone	0.397	-0.029	-0.150	-0.158	-1.649	0.642	-0.012	0.783	-0.834
NO_3^- -bearing	0.121	0.337	0.099	0.752	-0.228	0.679	-	2.949	0.492
NO_3^- -free	0.364	0.670	0.319	0.378	1.998	0.297	-3.158	0.970	0.452

Table S5. Lambda values of the Box-Cox transformed variables.

Data set	Lamda values				
	SRC	SRC_C	SRC_S	aF_{SRC}	SFC
Whole data set	-0.024	-0.050	0.132	0.155	0.176
FFA	-0.185	-0.191	-0.291	0.326	0.187
GKA	0.039	-0.052	0.685	-0.139	0.193
non-sulphidic	1.493	1.043	-0.054	0.095	-0.014
sulphidic	0.229	0.159	0.941	-0.313	0.117
transition zone	-0.159	-0.158	-1.650	-0.089	-0.152
NO_3^- -bearing	0.797	0.745	-0.307	0.069	0.120
NO_3^- -free	0.492	0.375	1.914	-0.266	0.344

235

240

245

References:

- 250 Addy, K., Kellogg, D. Q., Gold, A. J., Groffman, P. M., Ferendo, G., and Sawyer, C.: In situ push-pull method to determine ground water denitrification in riparian zones, *J. Environ. Qual.*, 31, 1017-1024, 2002.
- Altman, D. G. and Bland, J. M.: Measurement in Medicine - The analysis of method comparison studies, *Statistician*, 32, 307-317, 1983.
- 255 Bland, J. M. and Altman, D. G.: Applying the right statistics: Analyses of measurement studies, *Ultrasound in Obstetrics & Gynecology*, 22, 85-93, 2003.
- Bland, J. M. and Altman, D. G.: Comparing methods of measurement - Why plotting difference against standard method is misleading, *Lancet*, 346, 1085-1087, 1995.
- Bland, J. M. and Altman, D. G.: Statistical methods for assessing agreement between two
260 methods of clinical measurement, *Lancet*, 1, 307-310, 1986.
- Eschenbach, W. and Well, R.: Online measurement of denitrification rates in aquifer samples by an approach coupling an automated sampling and calibration unit to a membrane inlet mass spectrometry system, *Rapid Commun. Mass Spectrom.*, 25, 1993-2006, 2011.
- 265 Kana, T. M., Darkangelo, C., Hunt, M. D., Oldham, J. B., Bennett, G. E., and Cornwell, J. C.: Membrane inlet mass-spectrometer for rapid high-precision determination of N₂, O₂, and Ar in environmental water samples, *Anal. Chem.*, 66, 4166-4170, 1994.